Appendix A: Data processing

After collecting the data, the series from different data providers were harmonized and put into a common data format. This included converting all station coordinates into latitude and longitude. In a few cases when only station name and elevation were available but no coordinates, the missing coordinates were extracted from Google Maps using the approximate location (with correct elevation) based on the station name. Most data providers used station identifiers along with station names. We chose to have unique identifiers for all stations based on the station name. Station names were standardized by replacing blanks and apostrophes with underscores and by removing accents. If multiple stations had the same name within one data source, i.e. by data provider, the names were suffixed with the station identifier from the data provider. If multiple stations had the same name across data providers, the names were suffixed with the data provider identifier.

A1 Merging of records

The final database included several cases in which snow measurements for the same location were stored as separate records since they covered different periods and/or a slight relocation of the same station site occurred. In some cases, different records were available at very close locations where snow data were collected at the same time or over partially overlapping periods for different operative or research purposes. In order to maximize the temporal continuity and extent of available HS and HN series, the records referring to the same site or to very close locations were merged; one series was created from the multiple series by replacing missing values or missing periods. In particular, the merging was performed only if the sites were closer than 3 km and their vertical distance was less than 200 m. In the case of overlapping periods, the data from the series with the fewest gaps were retained. The merging was evaluated and performed on HS series first. In the case that HN series for the same sites were also available, the data were merged by following the same criteria used for HS in order to preserve consistency between HS and HN measurements. The metadata of the most recent series included in the merging were assigned to the resulting record. About 60 merged series were obtained in total, and the duplicate records for the same site were discarded.

A2 Quality control

The series were quality checked in order to remove recording errors. First, below zero HS or HN values were replaced with missing values. Then a temporal consistency check was applied to HS to identify recording errors. Series were screened for jumps larger than 50 cm (up and down on 2 consecutive days, or vice versa). This criterion identified 680 values from the daily observations from all series, which were checked manually, and recording errors were replaced with missing values. Another issue with HS series is that missing observations might falsely be recorded as 0 cm. To identify suspicious series, mean winter (December to February) HS and the fraction of 0 cm values were calculated per station. Then, looking at a surrounding elevation band per station (200 to 500 m, depending on the elevation and station availability), series were marked if the mean HS was less than the 5th percentile or the fraction of 0 cm values was higher than the 95th percentile of all stations in the elevation band. Given the climatological nature of this pre-screening and the stronger dependence on elevation, we did not consider horizontal distance for this step. This resulted in 181 suspicious series which were checked manually. For 32 stations, there were periods when 0 cm was obviously a missing value, and in these periods, the 0 cm values were replaced with missing values; the remaining 149 stations had no missing values denoted as 0 cm. Finally, during all previous manual checks, series that showed "dubious" behaviour were marked, which were in total 48 series. Dubious behaviour was, for example, an inconsistency between HN and HS, unlikely values, improbable temporal variability, multiple seasons with no snow, or excessive gaps. From these 48 series, 29 were considered usable, 11 had some periods removed, and 8 were completely removed.

These procedures could identify some errors but definitely not all. Because of the large number of series, it was not feasible to manually quality check all of them, and fully automatic checks are often not feasible. Instead, a spatial consistency check was applied (see Appendix A.4), and the rest of remaining errors could be considered noise given the large amount of data.

A3 Gap filling

Most series contained gaps ranging from some days up to whole seasons. In order to conduct climatological or trend analyses, gaps in the series needed to be filled. For this, we employed a spatial interpolation approach which is similar to the one used for temperature and precipitation records (see, e.g., Brunetti et al., 2006; Crespi et al., 2018; Golzio et al., 2018). The approach is based on correlations between the series, and because snow strongly depends on elevation, we first performed a spatial analysis to identify which correlations can be expected depending on horizontal and vertical distances between stations. For this, pairwise correlations (Pearson) between the daily HS series were performed for December to April from 1981 to 2010 only if the series had at least 70 % valid data and only if each pair had at least 50 % of data in common. As expected, correlations decreased with both horizontal and vertical distance (Fig. A1), but correlations remained high even for large distances; e.g. correlations higher than 0.7 were found for vertical distances of up to 500 m (with less than 100 km horizontal distance) or

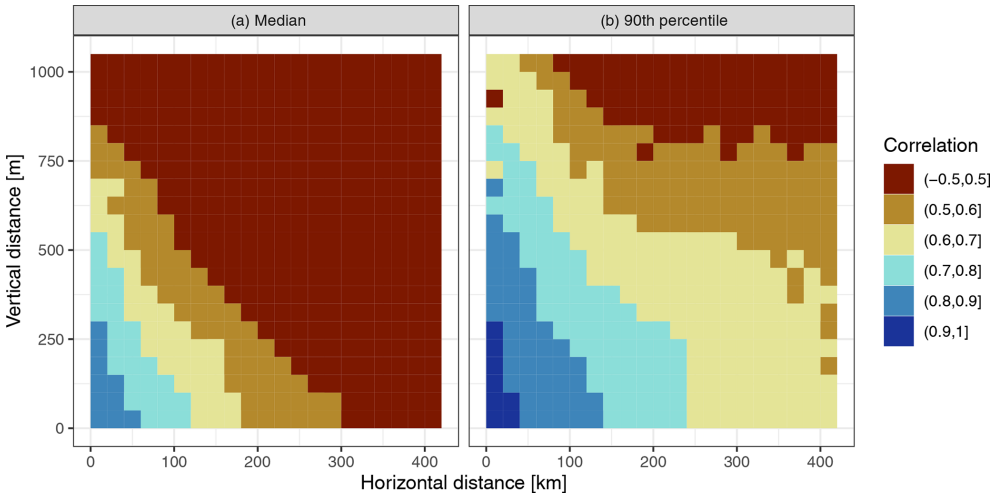

Figure A1. Summary of pairwise correlations between HS series for December to April, 1981 to 2010. The average (median, **a**) and 90th percentile **(b)** are shown of all pairwise correlations in bins of 20 km horizontal distance by bins of 50 m vertical distance. The correlations were only calculated if each series had at least 70 % valid data in the period and if each pair had at least 50 % of data in common.

horizontal distances of up to 200 km (with less than 250 m vertical distance). It should be noted that correlations can be high even if there are large differences in amounts or ratios between the series as long as the differences and ratios are constant across the range of values.

The chosen approach fills a gap based on finding neighbouring series that are highly correlated to the one with gaps. The gap-filling algorithm works as follows for each gap.

1. Find temporally surrounding non-missing values in the gap series around the gap date ("window data"); see also Fig. A2a.
   - 1.1. Take 15 d before and after the gap. This results in 31 d of the year; e.g. for 16 January, this would be 1 to 31 January and for 1 January, this would be 16 December to 17 January.
   - 1.2. Repeat step 1.1 for 10 years before and after the gap. This results in 21 years; e.g. for 1996, this would be 1986 to 2006.
   - 1.3. This window data potentially contains 651 values ($21 \cdot 31$) but likely has missing values. If there are more than 150 non-missing values, continue to step 2. If there are less than 150 non-missing values, increase the day window by 5 d in both directions, and repeat from 1.1. If the day window has reached 45 in one direction (i.e. a total of 91 d) and still there are less than 150 non-missing dates, stop. Note that only the day window is increased, the year window from 1.2 stays constant at 10 years before and after.
2. Pre-select potential reference series (Fig. A2b) based on the following criteria: vertical distance to gap series is below 500 m, horizontal distance is below 200 km, and the value at the date of the gap is not missing.
3. For each potential reference series, do the following.
   - 3.1. Identify dates with values available for both gap and reference series in the window identified in step 1 (Fig. A2c). Continue only if more than 80 % of the minimum 150 non-missing values (i.e. 120) are available in common.
   - 3.2. For the common dates, calculate mean of gap series and mean of reference series, and calculate correlation between gap series and reference series. If all values of gap and reference series are zero, set the correlation to the minimum threshold (see step 4) plus 0.001 (in order to be able to fill also zero periods). If only one of the series has all zero values, i.e. either gap or reference but not both, set the correlation to zero.
   - 3.3. Calculate ratio between mean of gap series divided by mean of reference series. If the mean of the reference series (divisor) is zero, set the ratio to zero (in order to be able to fill also zero periods).
4. Sort potential reference series by correlation with gap series (from step 3.1). Remove all candidates with a correlation below 0.7. This threshold was chosen as it is used, for example, in the homogenization of snow depth (Marcolini et al., 2017a).
5. Select the first five best correlated reference series or up to five, depending on how many are available.
6. Calculate weights based on vertical distance. The weights are based on exponential decay with a halving distance of 250 m ("half-time" transformation of decay constant). This implies that the weights are halved every 250 m.

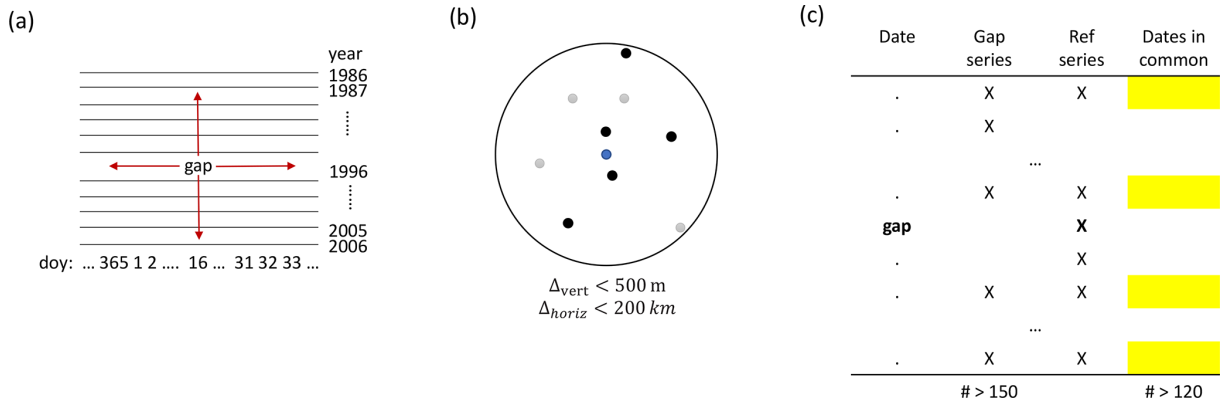

Figure A2. Visualization of some steps of the gap-filling algorithm. Panel **(a)** shows how the window data in the gap series around the gap is determined (step 1); doy is day of the year. Panel **(b)** shows the selection of potential reference series by horizontal and vertical distance (step 2). Panel **(c)** shows how common dates for gap and reference series are identified (step 3); the dates come from the window in **(a)**.

7. Fill the gap value with a weighted (step 6) average of the reference series values adjusted by the ratios between gap and reference series (step 3.3): $\mathrm{HS}_t^{\mathrm{gap}} = \frac{1}{n}\sum_{i=1}^{n} w_i \cdot \mathrm{HS}_t^{\mathrm{ref}_i} \cdot \frac{\mathrm{HS}_{\mathrm{mean}}^{\mathrm{gap}}}{\mathrm{HS}_{\mathrm{mean}}^{\mathrm{ref}_i}}$, where t is the date of the gap, i is the index of the reference series, n is the number of the reference series 1…5, and w_i are the weights with $\sum_i w_i = 1$.

The filled value was rounded to the nearest integer value in centimetres. Since the method requires finding suitable reference stations, it was only performed for the period 1961 to 2020 because the station density was too low before. The gap filling was applied to all gaps in all series considering all available data; afterwards, thresholds were applied to select usable series (see end of this section).

The chosen limits of 200 km horizontal distance and 500 m vertical distance might seem very high in the Alpine context with the complex topography. Since we were interested in larger-scale snow patterns and not local snow peculiarities, such large distances are justified. Moreover, the correlation threshold should exert control on selecting only stations that share the same snow cover evolution, and high correlations were found up to these horizontal and vertical limits (Fig. A1). On the other hand, a nearby station might also be a worse predictor than a more distant one, if, for example, it differs in its local climate.

Since this gap-filling approach has not yet been used for snow depth, we performed a cross-validation analysis to identify the gap-filling errors. For this, we used data from November to May from the period 1981 to 2010. For each station and each year, 1 month at a time was held out but only if at least 10 d were available. Thus, for each month, a maximum potential of ∼900 values were cross-validated; however, the effective number was lower because of missing values and because not all gaps could be filled if no suitable reference stations were available. In order to test the effect of shorter period gaps, we also applied the cross-validation to subsets (to reduce computation time): (1) 100 random samples of 1 d and (2) 20 random samples of 5 consecutive days. Then, the held-out values were filled using the above approach, and metrics were calculated based on the filled and held-out values. Metrics include the bias, the MAE (mean absolute error), the MAE for non-zero held-out values only, and a modified version of relative MAE. The relative MAE is based on the MAE for non-zero values only, and this non-zero MAE is divided by the average of the held-out non-zero values. This is then not a "true" relative error which would divide each error by the true value, i.e. $\frac{1}{n}\sum_{i=1}^{n}|\frac{y_i - x_i}{x_i}|$, but our modification is $\frac{1}{n}\sum_{i=1}^{n}\frac{|y_i - x_i|}{|\underline{x}|}$, where $\underline{x}$ is the average of all x_i. This was done to remove the large influence of errors close to zero which are not that relevant in this case. The metrics were only calculated if more than 50 values were available per month and station (out of potentially ∼900 for the month-long gaps and 100 for the 1 and 5 d gaps) in order to provide robust estimates.

The cross-validation showed that the gap filling has extremely little bias (Table A1), with the overall average daily bias for the month-long gaps being −0.04 cm. Average daily MAE for filling whole months was 1.6 cm (averaged over stations located at 0–1000 m), 7.7 cm (1000–2000 m), and 22.0 cm (2000–3000 m). MAE was lower for 1 and 5 d long gaps compared to month-long gaps, but almost no differences were observed comparing 1 or 5 d, e.g. for the 1000–2000 m band. MAE for 1 d gaps was 6.2 cm and for 5 d gaps 6.4 cm compared to 7.7 cm for 1 month gaps. The relative MAE of month-long gaps decreased with elevation from 39.4 % (0–1000 m) to 32.7 % (1000–2000 m) to 22.8 % (2000–3000 m). Additionally, there was also a seasonal dependence of MAE, while the bias remained largely constant across the season (Fig. A3). MAE below 2000 m peaked in February, while above 2000 m, MAE increased throughout the season. Relative MAE decreased with higher snow depths both temporally and with elevation; that is, relative MAE was lowest in

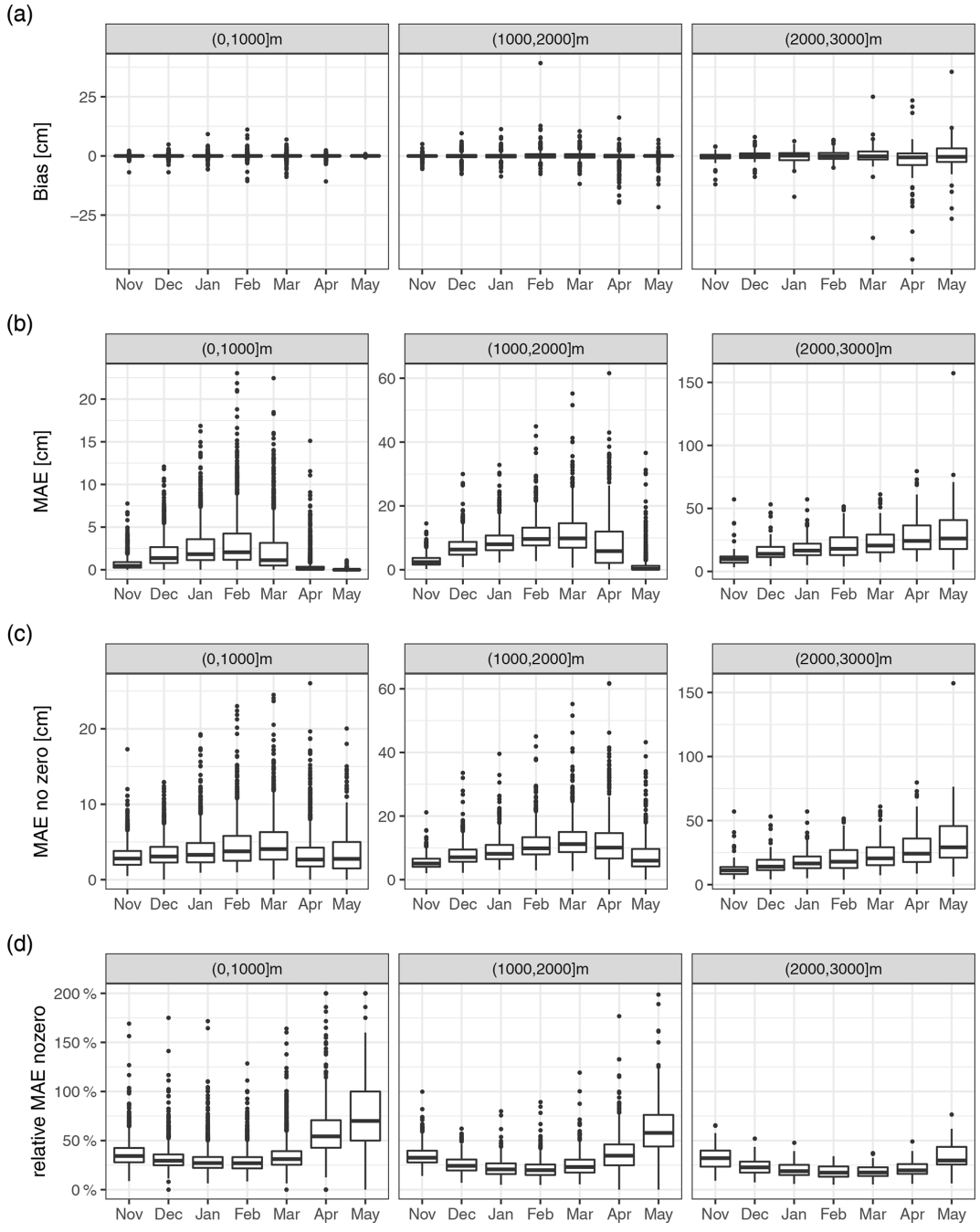

Figure A3. Cross-validation metrics for the gap-filling approach: **(a)** bias, **(b)** mean absolute error (MAE), **(c)** mean absolute error for non-zero values (MAE no zero), and **(d)** non-zero MAE divided by the true non-zero mean (relative MAE no zero). Panels show the 1000 m elevation bands indicated in the title. The boxplots represent statistical quantities. The box indicates the first and third quartile, the bold line inside the box is the median, the vertical lines outside the box extend up to the most extreme point but at most 1.5 times the interquartile range (IQR; height of the box), and, finally, points below and above $1.5 \cdot \mathrm{IQR}$ of the first and third quartile are shown as separate points.

February and at high elevations. It is to be expected that errors at the end of the season are related to the ablation scheme (i.e. local climatic and topographic characteristics that influence ablation) of the different stations; however, at this stage, we did not check this issue further.

Moreover, we compared our proposed gap-filling approach to results from gap-filling snow depth series using simulations of the Crocus snow model for the French Alps. The Crocus simulations with meteorological forcing were performed independently of this study, but we found it useful

Table A1. Cross-validation (CV) metrics for the gap-filling approach: bias (the difference between gap-filled and observed values), the mean absolute error (MAE), mean absolute error only for non-zero observed values (MAE no zero), and MAE no zero divided by the average of all true non-zero values (Rel. MAE no zero).

Elevation band (m)	CV period	Bias (cm)	MAE (cm)	MAE no zero (cm)	Rel. MAE no zero
(0,1000]	1 d	−0.0	1.3	3.1	30.1 %
	5 d	−0.0	1.4	3.3	34.0 %
	1 month	−0.0	1.6	3.9	39.4 %
(1000,2000]	1 d	−0.1	6.2	7.9	26.1 %
	5 d	−0.1	6.4	8.2	28.5 %
	1 month	−0.1	7.7	9.7	32.7 %
(2000,3000]	1 d	−0.6	18.2	18.6	18.9 %
	5 d	−0.8	18.3	18.7	19.2 %
	1 month	−0.4	22.0	22.5	22.8 %

to compare the two approaches – albeit only exploratively. The observed snow depths with gaps were assimilated into the Crocus modelling scheme using SAFRAN reanalysis data as forcing (López-Moreno et al., 2020). The two gap-filling approaches were compared only for existing gaps in the French Alps. This was intended as a preliminary companion evaluation, and no cross-validation was performed. Thus, there was no ground truth to evaluate the two gap-filling approaches with formal metrics, and we only performed a visual assessment (figures for comparison available in Matiu et al., 2020). Time series of both gap-filling procedures looked remarkably similar even for reconstructions of complete missing seasons; the different snowfall events were visible in both, and snow depths averaged over multiple days were comparable. Differences emerged in the snow settling behaviour and for the spring snow melting periods. More information on this exercise is available from the authors on request.

For Switzerland, a comparison of gap-filling methods for HS was performed which aimed at reconstructing complete missing seasons and which included regression-based methods and snow models (Aschauer et al., 2020). While our proposed method was not explicitly used in that comparison, it can be assumed to be similar to the regression-based and distance-weighted methods used there. The errors reported in their study (root mean squared error less than 20 cm) are in the same order of magnitude as those found in our cross-validation.

Altogether, the above-mentioned points (the cross-validation results, the comparison to Crocus, and the preliminary findings of the Swiss study) convinced us that the gap-filling procedure is also suitable for reconstructing whole seasons and not only some intermediate gaps, considering the fact that we only used it to derive monthly means (see below) and did not use the daily values directly. Further research would be required to check the suitability of the daily reconstructions, in our opinion, also considering the temporal distance to the last existing observations. For the final analysis, all gap-filled data within the recording period was used, and we also allowed the period to be extended by up to 5 years before the start or after the end of the recordings – but only if the total number of gap-filled observations was less than the number of observations without gap filling. The main reason for this extension was to have series covering the complete period until 2019 because some series stopped just a few years earlier. As a sensitivity analysis, we repeated most of the statistical analysis also for the original data without gap filling and provide results in the Supplement; the estimated modes of variability matched (Fig. S12 in the Supplement), the magnitude and variability in monthly trends were similar, although significantly fewer stations were available (Fig. S10 in the Supplement), and finally the time series of 500 m average HS also showed similar behaviour (Fig. S11 in the Supplement). The gap filling was able to significantly increase the temporal availability, but its aim was not to fill all gaps. Gaps were not filled, for example, if no suitable reference station was found or if not enough common data were available.

A4 Aggregation and spatial consistency

The daily snow depth (HS) values were aggregated to mean monthly HS if at least 90 % of the daily values were available in the respective months after the gap filling (monthly time series plots available at Matiu et al., 2020).

Based on the monthly series, a consistency check was performed (Crespi et al., 2018) which identified dubious values and/or series (but can also identify series with strong local influences on snow depth). Each monthly HS series of the tested station was reconstructed from up to five reference stations by a spatial interpolation approach. The reference series were selected if the monthly record was available and if at least 10 monthly records were in common with the tested station. If more than five neighbours were available, the ones with the highest weights were selected with weights being derived from the horizontal distance and eleva-

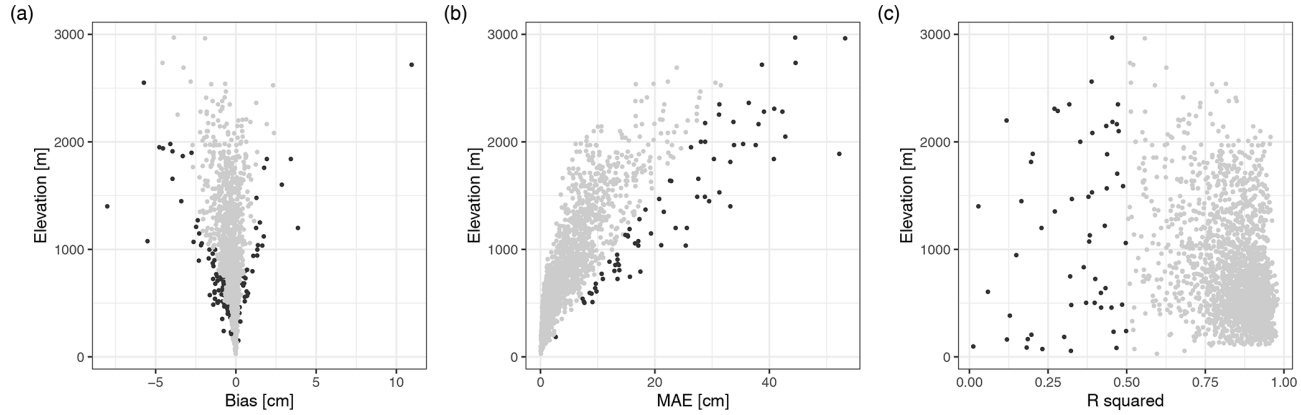

Figure A4. Metrics for spatial consistency: **(a)** bias, **(b)** mean absolute error (MAE), and **(c)** R^2 (squared correlation). Metrics were derived from statistical simulations of the monthly series from December to February using spatial neighbours. Black points indicate stations which were further analysed with manual checks.

tion difference, which is similar to the gap-filling procedure described above. Each reference station value was rescaled by the ratio between tested and reference mean HS for the month under reconstruction. Finally, the monthly simulation of the tested series was defined as the median of up to five rescaled neighbouring values. The comparison between simulated and observed monthly HS series for each station was evaluated by computing bias, MAE, and R^2 (squared correlation) from December to February in order to avoid unreliable low error values due to zeros in HS records outside of winter.

The mean bias over all stations was −0.3 cm (min, max: −8.0, 10.9 cm), average MAE was 4.8 cm (0.1, 61.3 cm), and average R^2 was 0.83 (0.0, 0.98). However, there was a strong elevational dependency, and station metrics deteriorated with elevation (Fig. A4). A semi-automatic approach was considered to look for suspicious series. The following criteria were used to screen stations: bias outside the 95 % confidence interval per elevation band (250 m bands up to 1500 m, then 1500 to 2000 m, and 2000 to 3000 m), MAE above a manually defined threshold line (see Fig. A4b), R^2 below 0.5, or simulation not successful because of too many gaps. This yielded 225 stations which were checked manually by looking at monthly simulated and observed series and daily series. Only 14 stations were found suspicious and 18 partly suspicious; all of these 32 series were removed from the statistical analyses. More detailed results and time series comparing simulated with observed snow depths are available as auxiliary material (Matiu et al., 2020).

Appendix B: Additional figures and tables

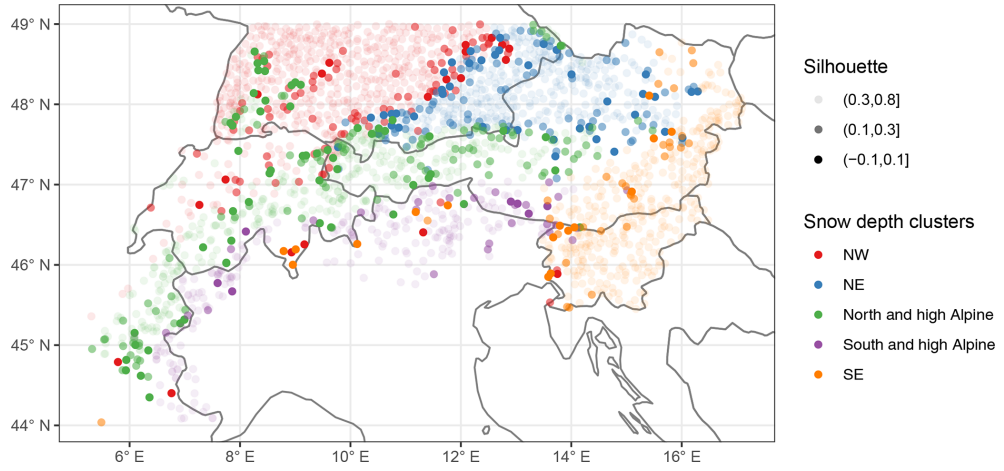

Figure B1. Silhouette values of the stations which show the consistency of clustering. The silhouette is a measure of how similar the station is to its own cluster compared to the other clusters (see Sect. 2.4). High values indicate a good match, while low and negative values indicate a poor match.

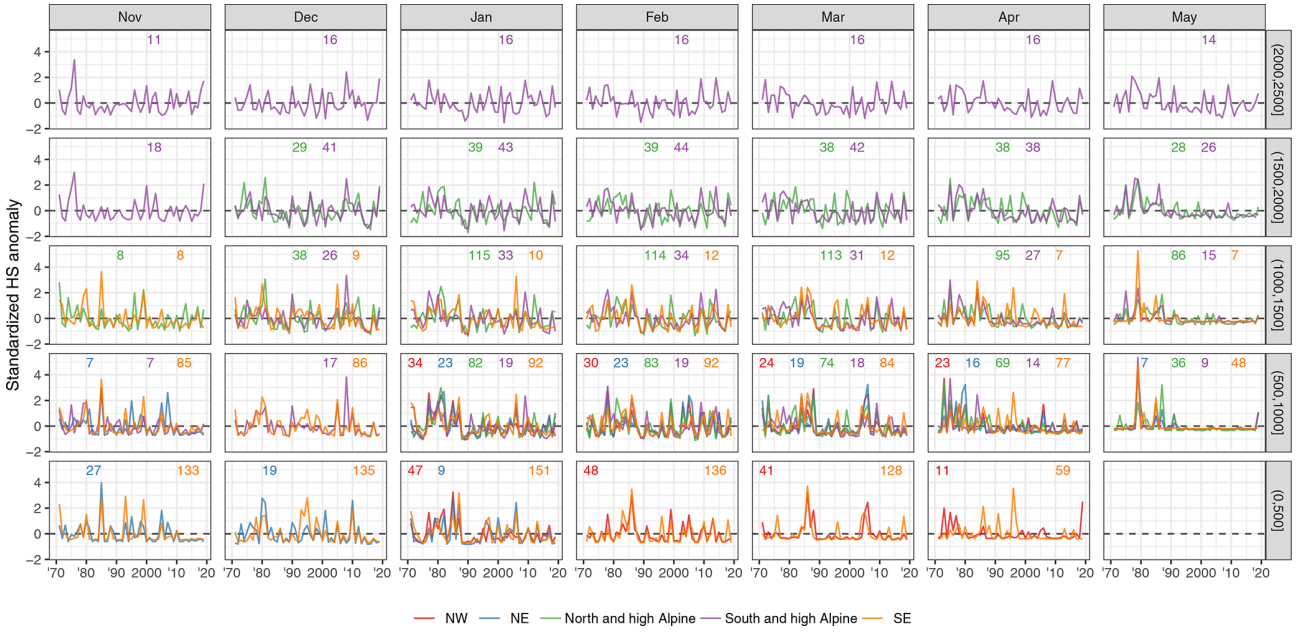

Figure B2. Same as Fig. 8 but using standardized anomalies.

https://doi.org/10.5194/tc-15-1343-2021

Table B1. Overview of the literature on snow cover trends in the European Alps.

Area	Number of stations	Time period	Season	Snow variable	Methods
(Bach et al., 2018) Mean HS −12.2 %/10 yr (40 % station $p < 0.05$); max HS −11.4 %/10 yr (36 % station $p < 0.05$); except coldest climates					
Pan-Europe: mostly Germany, Benelux, AT-Tirol, Czech Republic, Slovakia, Finland; partly UK, Balkan, partly east of Baltic Sea	(not specified)	1951–2017	DJF	Mean HS; Max HS (95 pctl)	OLS if trend pos.; OLS (exp) if trend negative; significance: Mann–Kendall
(Beniston, 2012b) 10 %–50 % decline in DJF HS (less of a decline in the moist north vs. dry south)					
Switzerland	10	1930–2010	DJF; NDJFMA	Mean HS; snow days (10 cm)	Visual; 5 yr moving window
(Durand et al., 2009) HS no trend at 2700 m, decreases below; n0 (number of days with snow) negative trends					
French Alps	Modelling: ERA-40, SAFRAN, Crocus	1959–2005	DJF	Mean HS $n0$ HS100d (minimum 100 d snow depth)	300 m elevation steps (1500–2700); Spearman correlation (year − $n0$); step-year ($n0$); linear trend ($n0$)
(Klein et al., 2016) SCD shorter 8.9 d per decade; more because of earlier snow melt (5.8 d per decade); decrease in maxHS and earlier date of maxHS					
Switzerland	11	1970–2015	Sep–Aug	maxHS; date of snow onset, snowmelt, maxHS; SCD; snow days (1, 20, 50, 100)	Theil–Sen, Mann–Kendall; stepwise regression
(Kreyling and Henry, 2011) 150 stations showed a decrease ($p < 0.05$ for 69) and 22 an increase ($p < 0.05$ for 1); decrease accelerated over the last 15 yr (-0.48 to $-0.89\,\mathrm{d\,yr^{-1}}$)					
Germany	177	1950–2000	Aug–Jul	SD (1 cm)	OLS; random effects with stations
(Laternser and Schneebeli, 2003) All variables show an increase until 1980, followed by a significant decrease; trends more pronounced at middle and low elevations; south = north; shorter SCD because earlier melt in spring					
Swiss Alps	140 (HS) 120 (HN)	1931–1999	NDJFMA; 2 month splits	Mean seasonal HS; SCD (start, end, length); days with HN > 0, 10,. . . ; HN3max (max 3 d HN)	Trend analysis; relative to long-term mean; trend of short period equal to long period

Table B1. Continued.

Area	Number of stations	Time period	Season	Snow variable	Methods
(Lejeune et al., 2019) 39 cm less in 1990–2017 vs. 1960–1990					
France	1 (Col de Porte)	1960–2017	DJFMA	mean HS	Moving window (15 yr) and comparison 30 yr
(Marcolini et al., 2017b) Different dynamics above and below 1650 m; larger reductions at lower elevations; strong change late 1980s					
Italy (BZ + TN)	37	1980–2009	NDJFMA	SCD (> 30 cm); seasonal HS	Homogenization; Hovmöller plots; wavelet analysis
(Marty, 2008) Regime shift at end of 1980s, no clear trend since then					
Switzerland	34	∼ 1931–2008	DJFM	Snow days (5, 30, 50 cm)	Mann–Kendall; shift detection
(Marty and Blanchet, 2012) 44 % of stations show significant decrease in HSmax, 32 % for HN3max; decrease in spread of HSmax					
Switzerland	18 (HSmax) 25 (HN3max)	1931–2010	Annual	HSmax (annual max HS); HN3max (annual max sum HN 3 d)	Generalized extreme value model with time-dependent location and shape
(Marty et al., 2017) SWE decline (independent of lat or long); stronger and more significant decrease in spring (−80 % to −10 % low to high elevations/60 years) than winter; winter: some positive non-significant at high elevation					
alpine-wide (AT, FR, DE, IT, CH)	54	1968–2012	Index values (spring and winter)	SWE (not continuously measured)	Mann–Kendall; Theil–Sen
(Micheletti, 2008) Positive anomalies until the end of the 1980s then shift to low snow amounts until beginning of 2000; some recovery but still below level of 1980s					
Italy (FVG)	8	1972–2007	Seasonal	sumHN, max of monthly meanHS	Time series (only descriptive); % anomalies w.r.t. 1972–2007
(Scherrer et al., 2013) Strong decadal variability; high values 1900–1920 and 1960–1970/80; lowest values end 1980/1990; increases/plateau in 2000s linked to temperature evolution					
Switzerland	9	1864–2009	Annual	MAXNS (max annual HN); NSS (sum annual HN); DWSF (days with snowfall)	Plots; 20 yr smooth; comparison to 71 other stations

https://doi.org/10.5194/tc-15-1343-2021

Table B1. Continued.

Area	Number of stations	Time period	Season	Snow variable	Methods
(Schöner et al., 2009) Largest HS in 1940s/50s; summer snow decreasing; interannual variability in winter precipitation closely related to HS (highest in 1940s/50s, strong decreases since → less extremes)					
Austria	1 (Sonnblick)	1928–2005	Monthly	HS	Visual
(Schöner et al., 2019) EOF groups AT–CH in seven regions; trend analysis based on first PC; strong trends in the south at ∼ 2000 m: up to $-12\,\mathrm{cm}\,10\,\mathrm{yr}^{-1}$; strongest trends at highest elevations; regional dependence of trends					
Switzerland and Austria	196 (139 passed QC)	1961–2012	NDJFMA	Seasonal HS and HN	MK test with lag1 pre-whitening; running trend approach; Sen slope; EOF for regionalization
(Terzago et al., 2010) More snow Nov–Dec, less Jan–Apr, disappeared in May					
Italy (Piemonte)	3	1971–2009	Monthly	HN, HS, snowy days (HN ≥ 1 cm)	1971–2000 vs. 2000–2009
(Terzago et al., 2013) Some maxima in 1940, 1950, 1960, absolute 1970, absolute minima 1990, then recovery; significant decrease in seasonal HS of 2–14 cm per decade; stronger decreases in north (considering elevation); changes not driven by precipitation changes; snowfall anticorrelated to North Atlantic Oscillation (NAO)					
Italy (west)	6	1926/1951–2010	DJF, MAM, NDJFMAM	Precipitation, days with precipitation, solid precipitation fraction, HN, snowy days (HN > 0), HS	Trend analysis; Mann–Kendall; spectral analysis
(Valt et al., 2008) Snow cover decreased 14 d (1991–2007 vs. 1960–1990), stronger < 1600 m (16 d) vs. > 1600 m (11 d); fresh snow decreased 1990–2000, then stationary (for all altitudes and months)					
Italy (east and west)	5 (west); 6 (east)	∼ 1920/1960–2007	Oct–May	Snow days (≥ 1 cm); sumHN	Visual
(Valt and Cianfarra, 2010) NDJFMA cumulated snowfall (CSF) shows −3 to $-40\,\mathrm{cm}\,10\,\mathrm{yr}^{-1}$ for all 18 stations from 1960 to 2009, SCD also all negative; breakpoint ∼ 1990 before decrease, after increase; strongest negative trend in spring and below 1500 m; negative trend related to precipitation decrease; PCA shows long-term negative trend					
Italy (east and west)	18	1950–2009	DJFMA; DJF; MA	SCD (> 1 cm); CSF (sum of new snow)	Split by 1500 m alt; OLS, Mann–Kendall; changepoint; PCA

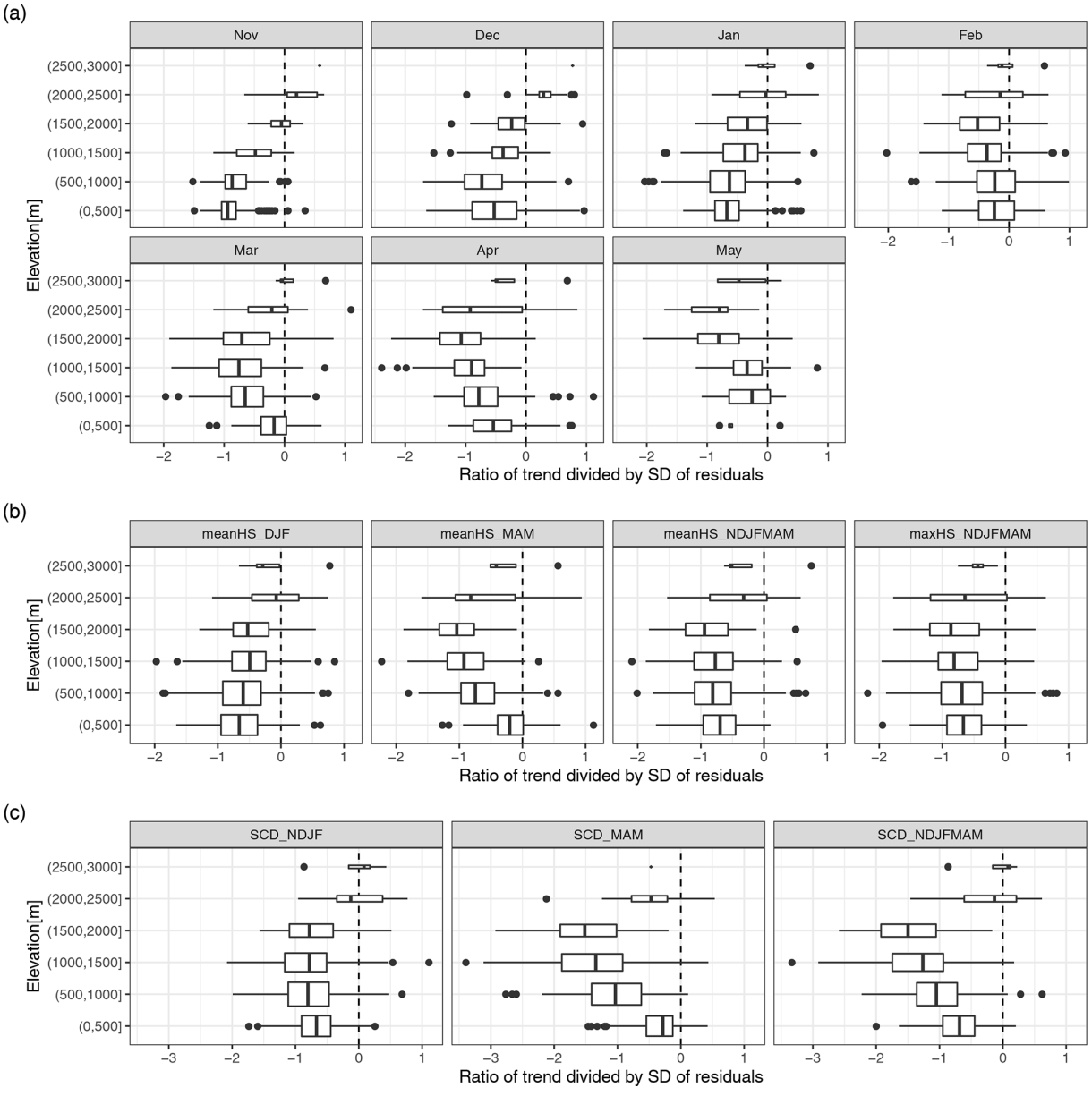

Figure B3. Ratio between the trend over the full period (1971 to 2019) and interannual variability (SD of the residuals). **(a)** The values for monthly mean HS (snow depth), **(b)** for seasonal indices of HS, and **(c)** for seasonal indices of SCD (snow cover duration). The boxplots represent statistical quantities. The box indicates the first and third quartile, the bold line inside the box is the median, the vertical lines outside the box extend up to the most extreme point but at most 1.5 times the interquartile range (IQR; width of the box), and, finally, points below and above $1.5 \cdot \mathrm{IQR}$ of the first and third quartile are shown as separate points. The height of the box is proportional to the number of observations in each group.

Table B2. Fraction of models with significantly positive or negative changes in the error variance by time. The remaining percentage (not shown) corresponds to the total of non-significant negative and positive changes. Empty cells indicate no stations with significant negative or positive trends (sig− and sig+). Changes were considered significant if the GLS model with a time coefficient for the error variance showed significantly improved goodness of fit compared to the OLS model with constant error variance ($p < 0.05$).

Region	Nov		Dec		Jan		Feb		Mar		Apr		May	
	sig−	sig+	sig−	sig+	sig−	sig+	sig−	sig+	sig−	sig+	sig−	sig+	sig−	sig+
NW					86.4 %		24.4 %	5.1 %	30.8 %	3.1 %	76.5 %	11.8 %		
NE	47.1 %	2.9 %	16.7 %		47.1 %	2.9 %	4.0 %	8.0 %	28.6 %	4.8 %	78.9 %		80.0 %	
N&hA	53.8 %		4.3 %		28.9 %	0.4 %	5.5 %	0.4 %	22.4 %		72.8 %		75.3 %	4.7 %
S&hA	43.9 %	4.9 %		26.7 %	8.0 %	8.0 %	9.1 %	6.4 %	14.0 %	6.5 %	41.1 %	1.1 %	76.6 %	1.6 %
SE	72.4 %	0.4 %	22.6 %	2.2 %	40.5 %	2.4 %	18.4 %	2.9 %	29.1 %	2.7 %	55.2 %	6.3 %	100.0 %	

Table B3. Overview of shareable data. The column "daily" indicates if the original daily data can be shared and "monthly" if the derived monthly data can be shared.

Code	Country	Data provider	Daily	Monthly
AT_HZB	Austria	HZB	No	Yes
CH_METEOSWISS	Switzerland	MeteoSwiss	No	Yes
CH_SLF	Switzerland	SLF	No	Yes
DE_DWD	Germany	DWD	Yes	Yes
FR_METEOFRANCE	France	Météo-France	Yes	Yes
IT_BZ	Italy	Bolzano	Yes	Yes
IT_FVG	Italy	Friuli Venezia Giulia	Yes	Yes
IT_LOMBARDIA	Italy	Lombardia	Yes	Yes
IT_PIEMONTE	Italy	Piemonte	No	No
IT_SMI	Italy	SMI	No	No
IT_TN	Italy	Trentino	Yes	Yes
IT_TN_TUM	Italy	Trentino (TUM)	No	No
IT_VDA_AIBM	Italy	Valle D'Aosta (AIBM)	No	No
IT_VDA_CF	Italy	Valle D'Aosta (CF)	Yes	Yes
IT_VENETO	Italy	Veneto	No	Yes
SI_ARSO	Slovenia	ARSO	No	Yes

Appendix C: Seasonal snow indices

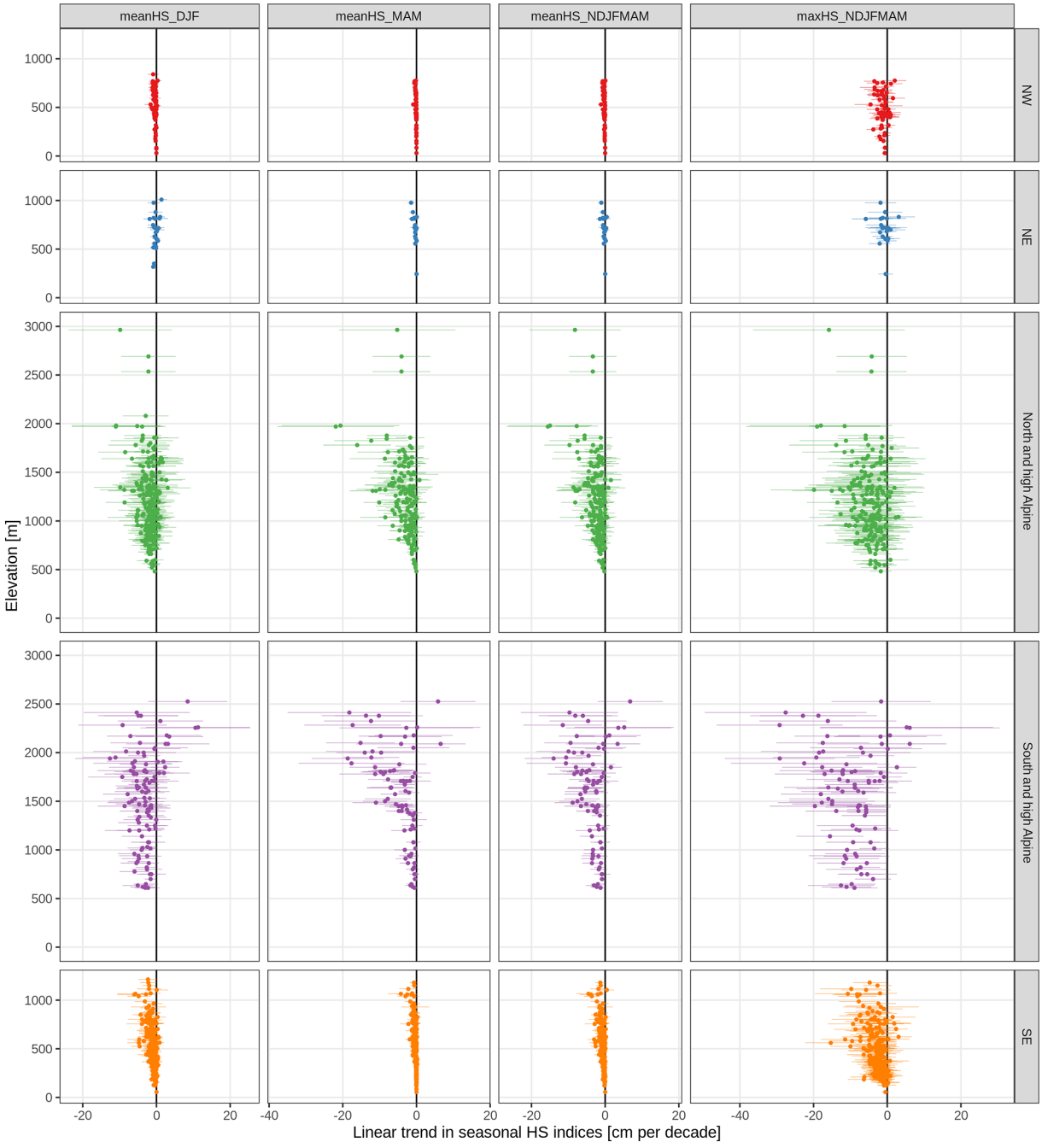

Figure C1. Long-term (1971 to 2019) linear trends in seasonal snow depth (HS) indices. Trends are shown separately by index (columns) and region (rows). The season is indicated in the columns with the first letter of the included months (e.g. DFJ is December, January, and February). Each point is one station. The points indicate the trend and the lines the associated 95 % confidence interval.

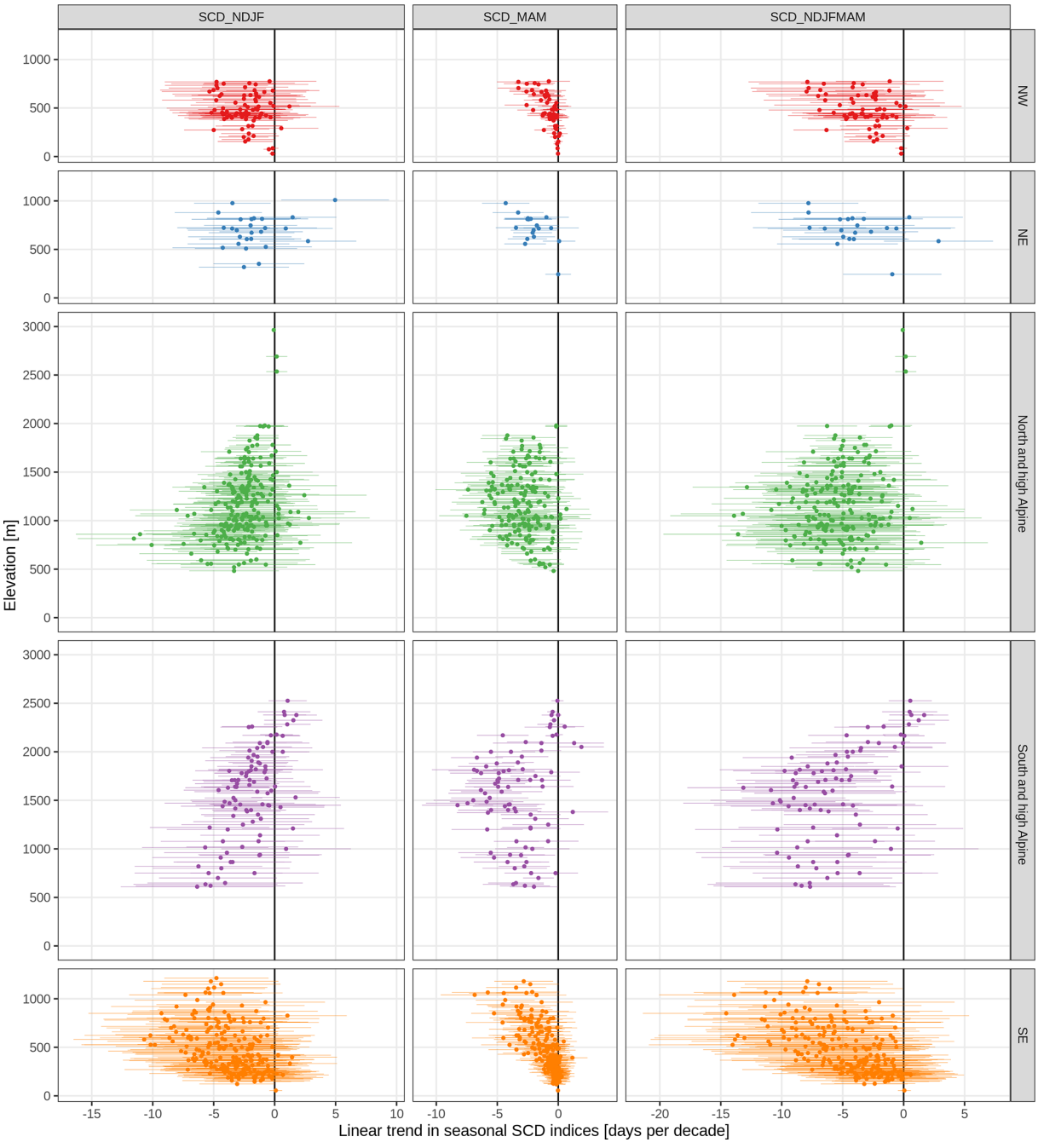

Figure C2. Long-term (1971 to 2019) linear trends in seasonal snow cover duration (SCD) indices. Trends are shown separately by index (columns) and region (rows). The season is indicated in the columns with the first letter of the included months (e.g. NDFJ is November, December, January, and February). Each point is one station. The points indicate the trend and the lines the associated 95 % confidence interval.

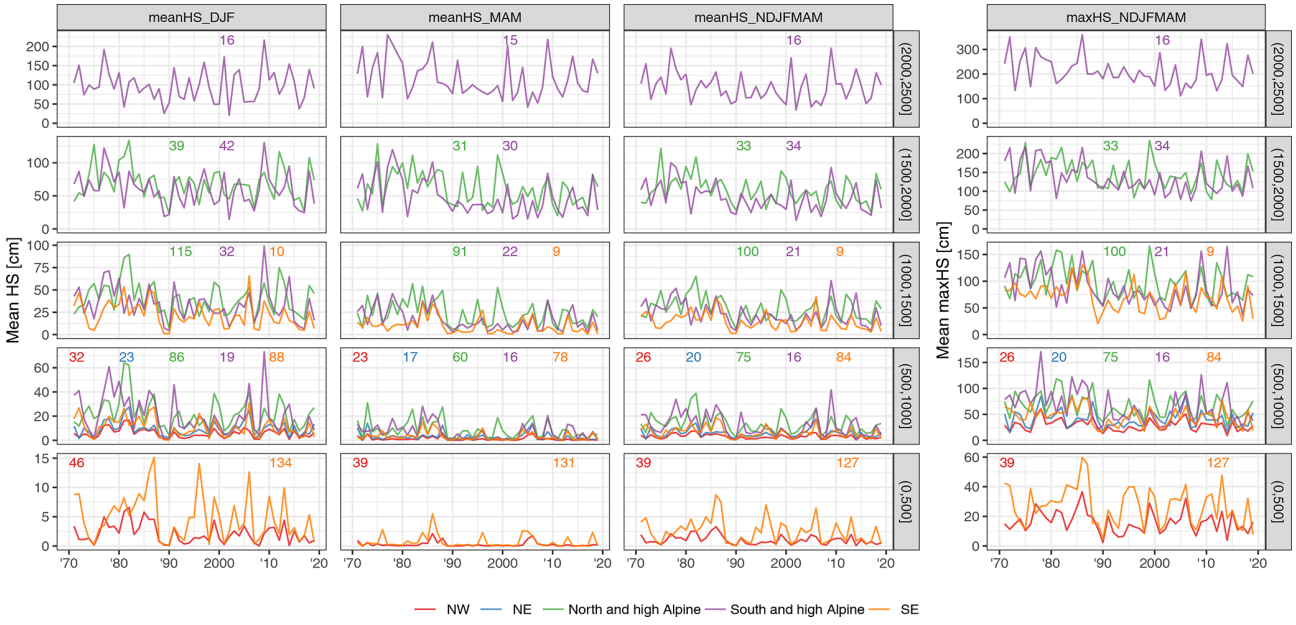

Figure C3. Time series of mean seasonal snow depth (HS) indices averaged by 500 m elevation bands. The rows indicate elevation band and the columns the index. The season is indicated in the columns with the first letter of the included months (e.g. DFJ is December, January, and February). The small numbers at the top of each panel denote the number of stations included in the average. Lines are only shown if more than five stations were available.

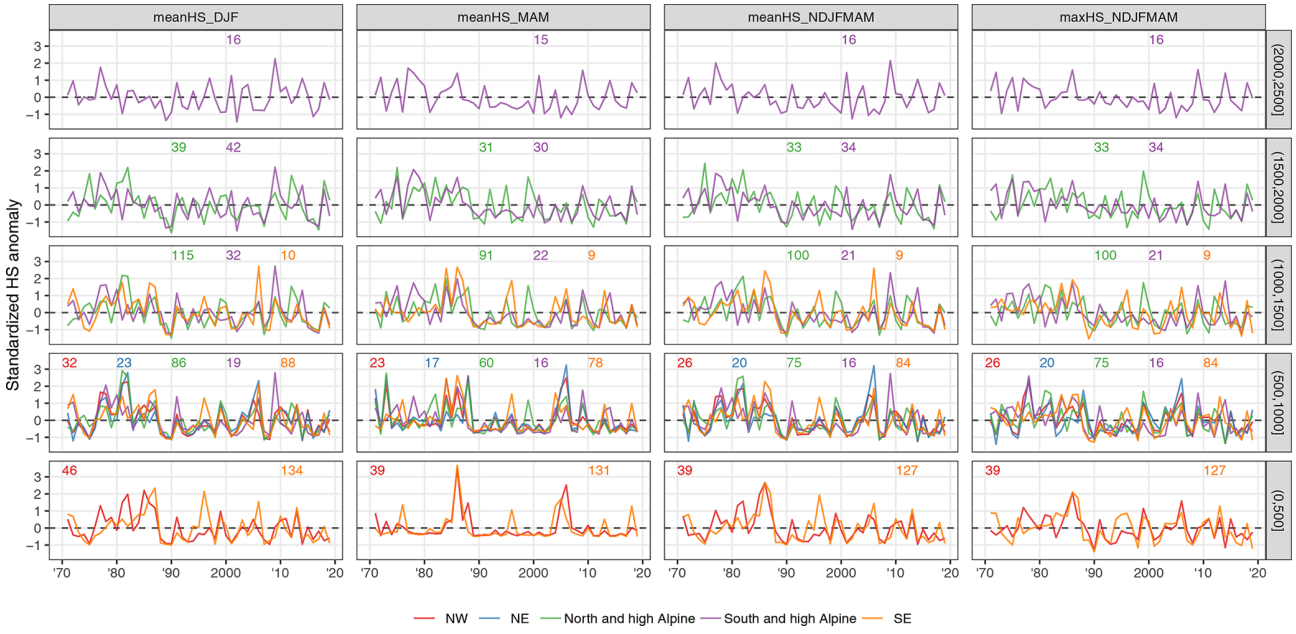

Figure C4. Same as Fig. C3 but for standardized anomalies.

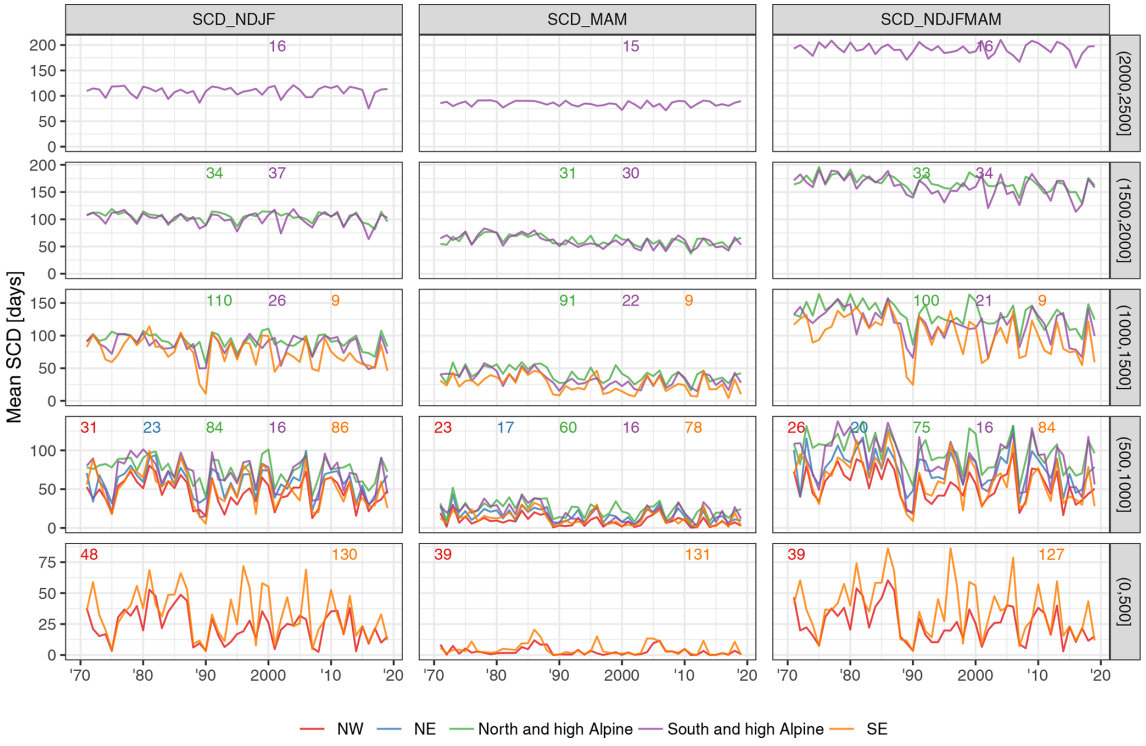

Figure C5. Time series of mean seasonal snow cover duration (SCD) indices averaged by 500 m elevation bands. The rows indicate elevation band and the columns the index. The season is indicated in the columns with the first letter of the included months (e.g. NDFJ is November, December, January, and February). The small numbers at the top of each panel denote the number of stations included in the average. Lines are only shown if more than five stations were available.

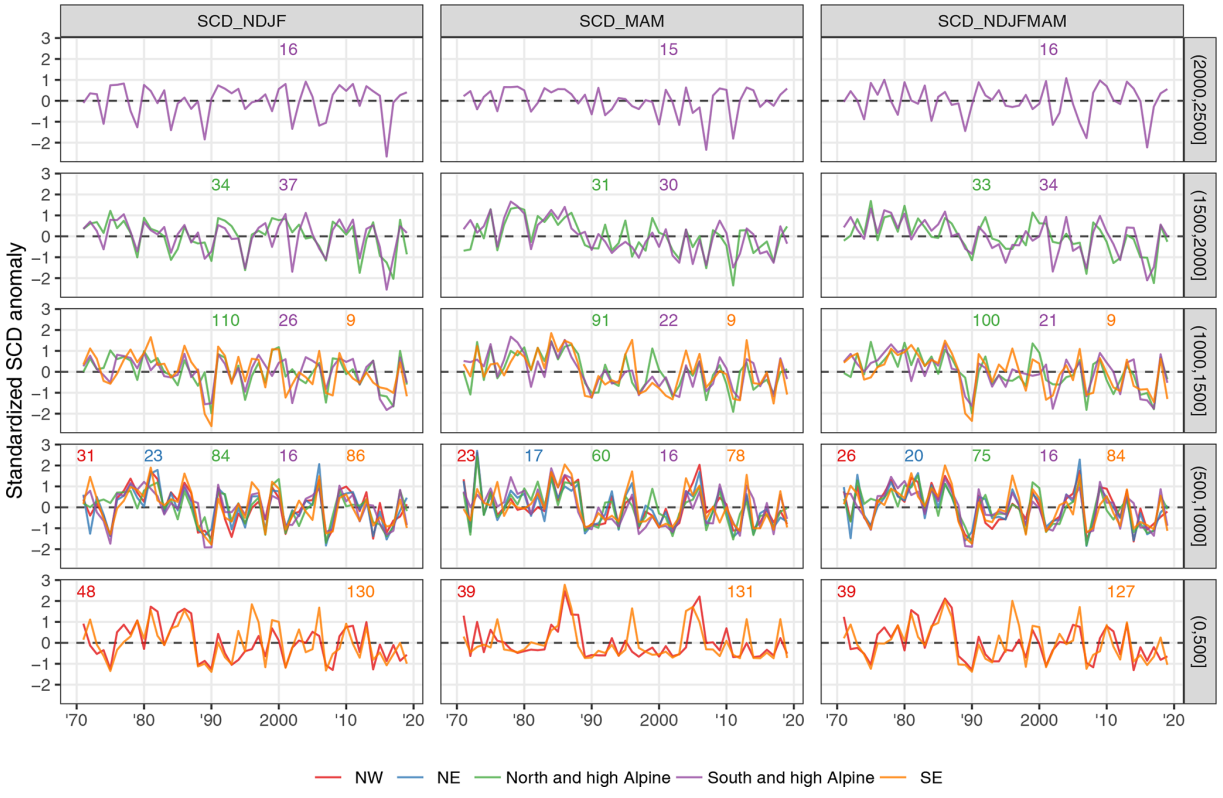

Figure C6. Same as Fig. C5 but for standardized anomalies.

Table C1. Overview of long-term (1971 to 2019) trends in mean seasonal snow depth indices. Summaries are shown by index, region, and 1000 m elevation bands (0 to 1000, 1000 to 2000, and 2000 to 3000 m). Cell values are the number of stations (#), the mean trend (mean, in cm per decade), and percentages of significant negative (sig−) and positive (sig+) trends; the remaining percentage (not shown) corresponds to the total of non-significant negative and positive trends. Empty cells denote no station available (for # and mean) and no stations with significant negative or positive trends (sig− and sig+). Trends were considered significant if $p < 0.05$. See also Fig. C1. A version of the table with 500 m bands instead of 1000 m is available in the Supplement (Table S6).

Index	Region	Elevation: (0,1000] m				Elevation: (1000,2000] m				Elevation: (2000,3000] m			
		#	mean	sig−	sig+	#	mean	sig−	sig+	#	mean	sig−	sig+
meanHS_DJF	NW	78	−0.38	26.9 %									
	NE	25	−0.26	8.0 %		1	1.36						
	N&hA	87	−1.64	14.9 %		154	−2.09	7.8 %		4	−4.28		
	S&hA	19	−3.57	42.1 %		74	−3.56	17.6 %		17	−0.07	5.9 %	
	SE	222	−0.95	22.1 %		10	−2.94	50.0 %					
meanHS_MAM	NW	62	−0.12	9.7 %									
	NE	18	−0.45	11.1 %									
	N&hA	61	−1.56	47.5 %		122	−3.74	42.6 %		3	−4.45		
	S&hA	16	−1.34	43.8 %		52	−5.38	69.2 %		16	−6.73	31.2 %	
	SE	209	−0.24	7.2 %	0.5 %	9	−1.82	33.3 %					
meanHS_NDJFMAM	NW	65	−0.23	41.5 %									
	NE	21	−0.31	9.5 %									
	N&hA	76	−1.44	32.9 %		133	−2.77	27.1 %		3	−4.96		
	S&hA	16	−2.15	56.2 %		55	−4.38	50.9 %		17	−2.91	23.5 %	
	SE	211	−0.60	27.0 %		9	−2.13	55.6 %					
maxHS_NDJFMAM	NW	65	−1.15	16.9 %									
	NE	21	−0.82	4.8 %									
	N&hA	76	−3.99	19.7 %		133	−5.19	20.3 %		3	−8.11		
	S&hA	16	−8.87	75.0 %		55	−10.33	56.4 %		17	−9.37	41.2 %	
	SE	211	−2.78	27.0 %		9	−6.59	55.6 %					

Table C2. Overview of long-term (1971 to 2019) trends in mean seasonal snow cover duration indices. Summaries are shown by index, region, and 1000 m elevation bands (0 to 1000, 1000 to 2000, and 2000 to 3000 m). Cell values are the number of stations (#), the mean trend (mean, in d per decade), and percentages of significant negative (sig−) and positive (sig+) trends; the remaining percentage (not shown) corresponds to the total of non-significant negative and positive trends. Empty cells denote no station available (for # and mean) and no stations with significant negative or positive trends (sig− and sig+). Trends were considered significant if $p < 0.05$. See also Fig. C2. A version of the table with 500 m bands instead of 1000 m is available in the Supplement (Table S7).

Index	Region	Elevation: (0,1000] m				Elevation: (1000,2000] m				Elevation: (2000,3000] m			
		#	mean	sig−	sig+	#	mean	sig−	sig+	#	mean	sig−	sig+
SCD_NDJF	NW	79	−2.47	30.4 %									
	NE	25	−1.92	16.0 %		1	4.96		100.0 %				
	N&hA	85	−3.33	38.8 %		144	−2.14	36.1 %		3	0.09		
	S&hA	16	−3.79	6.2 %		63	−2.08	28.6 %		17	−0.20		5.9 %
	SE	216	−3.67	28.2 %		9	−5.26	66.7 %					
SCD_MAM	NW	62	−0.82	22.6 %									
	NE	18	−2.05	66.7 %									
	N&hA	61	−2.56	59.0 %		122	−3.03	66.4 %					
	S&hA	16	−3.06	75.0 %		52	−4.16	78.8 %		16	−0.60	18.8 %	6.2 %
	SE	208	−0.99	20.7 %		9	−3.58	66.7 %					
SCD_NDJFMAM	NW	65	−3.33	40.0 %									
	NE	21	−3.86	33.3 %									
	N&hA	76	−5.58	57.9 %		133	−5.28	73.7 %		3	0.09		
	S&hA	16	−6.66	50.0 %		55	−6.67	80.0 %		17	−1.01	17.6 %	
	SE	211	−4.70	34.6 %		9	−8.84	88.9 %					

Code and data availability. All computations were performed with R statistical software version 4.0.2 (RCoreTeam, 2008). Colours for the figures were taken from scientific colour scales (Crameri, 2019) and colorBrewer. The code is available from a repository (https://doi.org/10.5281/zenodo.4064128, Matiu et al., 2020) which includes scripts for the following tasks: reading the different data sources, performing all data preprocessing, quality checking, gap filling, and statistical analyses.

Most data providers agreed to share their data; see Table B3 for the availability of daily and monthly values. For the full dataset, please contact the main authors (Michael Matiu or Alice Crespi); the usage is generally free for research purposes, although explicit consent is required from some data providers which want to keep track of the usage of the data. The shareable data are available from an open repository (https://doi.org/10.5281/zenodo.4064128, Matiu et al., 2020).

Supplement. The supplement related to this article is available online at: https://doi.org/10.5194/tc-15-1343-2021-supplement.

Author contributions. The study concept was defined by MM, AlC, GB, CM, SM, and WS. Involved in data curation were MM, AlC, GB, CMC, CM, DCB, GC, MV, WB, PC, GM, SCS, AnC, RC, AD, MF, MG, LM, JMS, AS, AT, SU, and VW. The formal analysis was performed by MM and AlC with input for methodology from CM, SM, and WS. The original draft was written by MM with assistance from AlC. The paper review and editing were performed by MM, AlC, GB, CMC, CM, SM, WS, GC, LDG, SK, BM, GR, ST, MV, PC, IG, GM, CN, SCS, US, MW, and LG.

Competing interests. The authors declare that they have no conflict of interest.

Acknowledgements. We thank the reviewers (two anonymous and Ross Brown) for their comments which have greatly improved the paper.

This project has received funding from the European Union's Horizon 2020 research and innovation programme under the Marie Sklodowska-Curie grant agreement no. 795310. This work has benefited from funding from the European Union's Horizon 2020 research and innovation programme under grant agreement no. 730203. CNRM/CEN is a member of LabEX OSUG@2020. Gabriele Chiogna acknowledges the support from the Stiftungsfonds für Umweltökonomie und Nachhaltigkeit GmbH (SUN) and likewise the support from the DFG (Deutsche Forschungsgemeinschaft) research group FOR2793/1 "Sensitivity of High Alpine Geosystems to Climate Change since 1850 (SEHAG)" grant CH981/3.

We acknowledge the E-OBS dataset from the EU-FP6 project UERRA (https://www.uerra.eu, last access: 5 March 2021) and the Copernicus Climate Change Service and the data providers for the ECA&D project (https://www.ecad.eu, last access: 5 March 2021). For providing us with station data, we are grateful to Günther Geier from the meteorological office and avalanche warning centre from the province of Bolzano, to Sara Ratto from the Centro Funzionale della Regione Autonoma Valle d'Aosta, and to Gregor Vertačnik from the meteorological office of the Slovenian Environmental Agency.

Financial support. This research has been supported by the European Commission Horizon 2020 Framework Programme CliRSnow (grant no. 795310) and PROSNOW (grant no. 730203) and the Deutsche Forschungsgemeinschaft (grant no. CH981/3).

Review statement. This paper was edited by Guillaume Chambon and reviewed by Ross Brown and two anonymous referees.

References

Aschauer, J., Bavay, M., Begert, M., and Marty, C.: Comparing methods for gap filling in historical snow depth time series, EGU General Assembly 2020, Online, 4–8 May 2020, EGU2020–17211, https://doi.org/10.5194/egusphere-egu2020-17211, 2020.

Auer, I., Böhm, R., Jurković, A., Orlik, A., Potzmann, R., Schöner, W., Ungersböck, M., Brunetti, M., Nanni, T., Maugeri, M., Briffa, K., Jones, P., Efthymiadis, D., Mestre, O., Moisselin, J.-M., Begert, M., Brazdil, R., Bochnicek, O., Cegnar, T., Gajić-Čapka, M., Zaninović, K., Majstorović, Ž., Szalai, S., Szentimrey, T., and Mercalli, L.: A new instrumental precipitation dataset for the greater alpine region for the period 1800–2002, Int. J. Climatol., 25, 139–166, https://doi.org/10.1002/joc.1135, 2005.

Auer, I., Böhm, R., Jurkovic, A., Lipa, W., Orlik, A., Potzmann, R., Schöner, W., Ungersböck, M., Matulla, C., Briffa, K., Jones, P., Efthymiadis, D., Brunetti, M., Nanni, T., Maugeri, M., Mercalli, L., Mestre, O., Moisselin, J.-M., Begert, M., Müller-Westermeier, G., Kveton, V., Bochnicek, O., Stastny, P., Lapin, M., Szalai, S., Szentimrey, T., Cegnar, T., Dolinar, M., Gajic-Capka, M., Zaninovic, K., Majstorovic, Z., and Nieplova, E.: HISTALP—historical instrumental climatological surface time series of the Greater Alpine Region, Int. J. Climatol., 27, 17–46, https://doi.org/10.1002/joc.1377, 2007.

Bach, A. F., Schrier, G. van der, Melsen, L. A., Tank, A. M. G. K., and Teuling, A. J.: Widespread and Accelerated Decrease of Observed Mean and Extreme Snow Depth Over Europe, Geophys. Res. Lett., 45, 12312–12319, https://doi.org/10.1029/2018GL079799, 2018.

Bazile, E., Abida, R., Verelle, A., Le Moigne, P., and Szczypta, C.: MESCAN-SURFEX surface analysis, deliverable D2.8 of the UERRA project, Technical Report, European Commission, available at: http://uerra.eu/publications/deliverable-reports.html (last access: 5 March 2021), 2017.

Beniston, M.: Impacts of climatic change on water and associated economic activities in the Swiss Alps, J. Hydrol., 412–413, 291–296, https://doi.org/10.1016/j.jhydrol.2010.06.046, 2012a.

Beniston, M.: Is snow in the Alps receding or disappearing?, WIREs Clim. Change, 3, 349–358, https://doi.org/10.1002/wcc.179, 2012b.

Beniston, M. and Stoffel, M.: Assessing the impacts of climatic change on mountain water resources, Sci. Total Environ., 493, 1129–1137, https://doi.org/10.1016/j.scitotenv.2013.11.122, 2014.

Beniston, M., Farinotti, D., Stoffel, M., Andreassen, L. M., Coppola, E., Eckert, N., Fantini, A., Giacona, F., Hauck, C., Huss, M., Huwald, H., Lehning, M., López-Moreno, J.-I., Magnusson, J., Marty, C., Morán-Tejéda, E., Morin, S., Naaim, M., Provenzale, A., Rabatel, A., Six, D., Stötter, J., Strasser, U., Terzago, S., and Vincent, C.: The European mountain cryosphere: a review of its current state, trends, and future challenges, The Cryosphere, 12, 759–794, https://doi.org/10.5194/tc-12-759-2018, 2018.

Bormann, K. J., Brown, R. D., Derksen, C., and Painter, T. H.: Estimating snow-cover trends from space, Nat. Clim. Change, 8, 924–928, https://doi.org/10.1038/s41558-018-0318-3, 2018.

Brown, R. D. and Petkova, N.: Snow cover variability in Bulgarian mountainous regions, 1931–2000, Int. J. Climatol., 27, 1215–1229, https://doi.org/10.1002/joc.1468, 2007.

Brunetti, M., Maugeri, M., Monti, F., and Nanni, T.: Temperature and precipitation variability in Italy in the last two centuries from homogenised instrumental time series, Int. J. Climatol., 26, 345–381, https://doi.org/10.1002/joc.1251, 2006.

Buchmann, M., Begert, M., Brönnimann, S., and Marty, C.: Evaluating the robustness of snow climate indicators using a unique set of parallel snow measurement series, Int. J. Climatol., 41, E2553–E2563, https://doi.org/10.1002/joc.6863, 2021.

Cornes, R. C., van der Schrier, G., Besselaar, van den E. J. M., and Jones, P. D.: An Ensemble Version of the E-OBS Temperature and Precipitation Data Sets, J. Geophys. Res.-Atmos., 123, 9391–9409, https://doi.org/10.1029/2017JD028200, 2018.

Crameri, F.: Scientific Colour Maps, Zenodo, https://doi.org/10.5281/zenodo.3596401, 2019.

Crespi, A., Brunetti, M., Lentini, G., and Maugeri, M.: 1961–1990 high-resolution monthly precipitation climatologies for Italy, Int. J. Climatol., 38, 878–895, https://doi.org/10.1002/joc.5217, 2018.

Durand, Y., Giraud, G., Laternser, M., Etchevers, P., Mérindol, L., and Lesaffre, B.: Reanalysis of 47 Years of Climate in the French Alps (1958–2005): Climatology and Trends for Snow Cover, J. Appl. Meteorol. Clim., 48, 2487–2512, https://doi.org/10.1175/2009JAMC1810.1, 2009.

Esposito, A., Engel, M., Ciccazzo, S., Daprà, L., Penna, D., Comiti, F., Zerbe, S., and Brusetti, L.: Spatial and temporal variability of bacterial communities in high alpine water spring sediments, Res. Microbiol., 167, 325–333, https://doi.org/10.1016/j.resmic.2015.12.006, 2016.

Gobiet, A., Kotlarski, S., Beniston, M., Heinrich, G., Rajczak, J., and Stoffel, M.: 21st century climate change in the European Alps—A review, Sci. Total Environ., 493, 1138–1151, https://doi.org/10.1016/j.scitotenv.2013.07.050, 2014.

Golzio, A., Crespi, A., Bollati, I. M., Senese, A., Guglielmina, A. D., Pelfini, M., and Maugeri, M.: High-Resolution Monthly Precipitation Fields (1913–2015) over a Complex Mountain Area Centred on the Forni Valley (Central Italian Alps), Adv. Meteorol., 2018, e9123814, https://doi.org/10.1155/2018/9123814, 2018.

Haberkorn, A.: European Snow Booklet – an Inventory of Snow Measurements in Europe, EnviDat, https://doi.org/10.16904/envidat.59, 2019.

Hock, R., Rasul, G., Adler, C., Cáceres, B., Gruber, S., Hirabayashi, Y., Jackson, M., Kääb, A., Kang, S., Kutuzov, S., Milner, Al., Molau, U., Morin, S., Orlove, B., and Steltzer, H.: High Mountain Areas, in: IPCC Special Report on the Ocean and Cryosphere in a Changing Climate, edited by: Pörtner, H.-O., Roberts, D. C., Masson-Delmotte, V., Zhai, P., Tignor, M., Poloczanska, E., Mintenbeck, K., Alegría, A., Nicolai, M., Okem, A., Petzold, J., Rama, B., and Weyer, N. M., in press, 2019.

IPCC: Summary for Policymakers, in: IPCC Special Report on the Ocean and Cryosphere in a Changing Climate, edited by: Pörtner, H.-O., Roberts, D. C., Masson-Delmotte, V., Zhai, P., Tignor, M., Poloczanska, E., Mintenbeck, K., Alegría, A., Nicolai, M., Okem, A., Petzold, J., Rama, B., and Weyer, N. M., in press, 2019.

Isotta, F. and Frei, C.: APGD: Alpine precipitation grid dataset, MeteoSwiss, Zurich-Airport, Switzerland, https://doi.org/10.18751/CLIMATE/GRIDDATA/APGD/1.0, 2013.

Isotta, F. A., Frei, C., Weilguni, V., Perčec Tadić, M., Lassègues, P., Rudolf, B., Pavan, V., Cacciamani, C., Antolini, G., Ratto, S. M., Munari, M., Micheletti, S., Bonati, V., Lussana, C., Ronchi, C., Panettieri, E., Marigo, G., and Vertačnik, G.: The climate of daily precipitation in the Alps: development and analysis of a high-resolution grid dataset from pan-Alpine rain-gauge data, Int. J. Climatol., 34, 1657–1675, https://doi.org/10.1002/joc.3794, 2014.

Keller, F., Goyette, S., and Beniston, M.: Sensitivity Analysis of Snow Cover to Climate Change Scenarios and Their Impact on Plant Habitats in Alpine Terrain, Climatic Change, 72, 299–319, https://doi.org/10.1007/s10584-005-5360-2, 2005.

Klein, G., Vitasse, Y., Rixen, C., Marty, C., and Rebetez, M.: Shorter snow cover duration since 1970 in the Swiss Alps due to earlier snowmelt more than to later snow onset, Climatic Change, 139, 637–649, https://doi.org/10.1007/s10584-016-1806-y, 2016.

Kreyling, J. and Henry, H. A. L.: Vanishing winters in Germany: soil frost dynamics and snow cover trends, and ecological implications, Clim. Res., 46, 269–276, https://doi.org/10.3354/cr00996, 2011.

Laternser, M. and Schneebeli, M.: Long-term snow climate trends of the Swiss Alps (1931–99), Int. J. Climatol., 23, 733–750, https://doi.org/10.1002/joc.912, 2003.

Lejeune, Y., Dumont, M., Panel, J.-M., Lafaysse, M., Lapalus, P., Le Gac, E., Lesaffre, B., and Morin, S.: 57 years (1960–2017) of snow and meteorological observations from a mid-altitude mountain site (Col de Porte, France, 1325 m of altitude), Earth Syst. Sci. Data, 11, 71–88, https://doi.org/10.5194/essd-11-71-2019, 2019.

Lencioni, V., Marziali, L., and Rossaro, B.: Diversity and distribution of chironomids (Diptera, Chironomidae) in pristine Alpine and pre-Alpine springs (Northern Italy), J. Limnol., 70, 106–121, https://doi.org/10.4081/jlimnol.2011.s1.106, 2011.

Leporati, E. and Mercalli, L.: Snowfall series of Turin, 1784–1992: climatological analysis and action on structures, Ann. Glaciol., 19, 77–84, https://doi.org/10.3189/S0260305500011010, 1994.

López-Moreno, J. I., Soubeyroux, J. M., Gascoin, S., Alonso-Gonzalez, E., Durán-Gómez, N., Lafaysse, M., Vernay, M., Carmagnola, C., and Morin, S.: Long-term trends (1958–2017) in snow cover duration and depth in the Pyrenees, Int. J. Climatol., 40, 6122–6136, https://doi.org/10.1002/joc.6571, 2020.

Mallucci, S., Majone, B., and Bellin, A.: Detection and attribution of hydrological changes in a large Alpine river basin, J. Hydrol.,

575, 1214–1229, https://doi.org/10.1016/j.jhydrol.2019.06.020, 2019.

Marcolini, G., Bellin, A., and Chiogna, G.: Performance of the Standard Normal Homogeneity Test for the homogenization of mean seasonal snow depth time series, Int. J. Climatol., 37, 1267–1277, https://doi.org/10.1002/joc.4977, 2017a.

Marcolini, G., Bellin, A., Disse, M., and Chiogna, G.: Variability in snow depth time series in the Adige catchment, J. Hydrol. Reg. Stud., 13, 240–254, https://doi.org/10.1016/j.ejrh.2017.08.007, 2017b.

Marcolini, G., Koch, R., Chimani, B., Schöner, W., Bellin, A., Disse, M., and Chiogna, G.: Evaluation of homogenization methods for seasonal snow depth data in the Austrian Alps, 1930–2010, Int. J. Climatol., 39, 4514–4530, https://doi.org/10.1002/joc.6095, 2019.

Marty, C.: Regime shift of snow days in Switzerland, Geophys. Res. Lett., 35, L12501, https://doi.org/10.1029/2008GL033998, 2008.

Marty, C. and Blanchet, J.: Long-term changes in annual maximum snow depth and snowfall in Switzerland based on extreme value statistics, Climatic Change, 111, 705–721, https://doi.org/10.1007/s10584-011-0159-9, 2012.

Marty, C., Tilg, A.-M., and Jonas, T.: Recent Evidence of Large-Scale Receding Snow Water Equivalents in the European Alps, J Hydrometeorol., 18, 1021–1031, https://doi.org/10.1175/JHM-D-16-0188.1, 2017.

Matiu, M., Crespi, A., Bertoldi, G., Carmagnola, C. M., Marty, C., Morin, S., Schöner, W., Cat Berro, D., Chiogna, G., De Gregorio, L., Kotlarski, S., Majone, B., Resch, G., Terzago, S., Valt, M., Beozzo, W., Cianfarra, P., Gouttevin, I., Marcolini, G., Notarnicola, C., Petitta, M., Scherrer, S. C., Strasser, U., Winkler, M., Zebisch, M., Cicogna, A., Cremonini, R., Debernardi, A., Faletto, M., Gaddo, M., Giovannini, L., Mercalli, L., Soubeyroux, J.-M., Sušnik, A., Trenti, A., Urbani, S., and Weilguni, V.: Snow cover in the European Alps: Station observations of snow depth and depth of snowfall (Version v1.1) [Data set], Zenodo, https://doi.org/10.5281/zenodo.4064128, 2020.

Micheletti, S.: Cambiamenti Climatici in Friuli–Venezia–Giulia, Neve e Valanghe, 63, 34–45, available at: https://issuu.com/aineva7/docs/nv63 (last access: 5 March 2021), 2008.

Najafi, M. R., Zwiers, F., and Gillett, N.: Attribution of the Observed Spring Snowpack Decline in British Columbia to Anthropogenic Climate Change, J. Climate, 30, 4113–4130, https://doi.org/10.1175/JCLI-D-16-0189.1, 2017.

Nitu, R., Roulet, Y.-A., Wolff, M., Earle, M., Reverdin, A., Smith, C., Kochendorfer, J., Morin, S., Rasmussen, R., Wong, K., Alastrué, J., Arnold, L., Baker, B., Buisán, S., Collado, J. L., Colli, M., Collins, B., Gaydos, A., Hannula, H.-R., Hoover, J., Joe, P., Kontu, A., Laine, T., Lanza, L., Lanzinger, E., Lee, G. W., Lejeune, Y., Leppänen, L., Mekis, E., Panel, J.-M., Poikonen, A., Ryu, S., Sabatini, F., Theriault, J., Yang, D., Genthon, C., van den Heuvel, F., Hirasawa, N., Konishi, H., Motoyoshi, H., Nakai, S., Nishimura, K., Senese, A., and Amashita, K.: WMO Solid Precipitation Intercomparison Experiment (SPICE) (2012–2015), World Meteorological Organization (WMO), available at: https://www.wmo.int/pages/prog/www/IMOP/publications-IOM-series.html (last access: 5 March 2021), 2018.

Notarnicola, C.: Hotspots of snow cover changes in global mountain regions over 2000–2018, Remote Sens. Environ., 243, 111781, https://doi.org/10.1016/j.rse.2020.111781, 2020.

Pepin, N., Bradley, R. S., Diaz, H. F., Baraer, M., Caceres, E. B., Forsythe, N., Fowler, H., Greenwood, G., Hashmi, M. Z., Liu, X. D., Miller, J. R., Ning, L., Ohmura, A., Palazzi, E., Rangwala, I., Schöner, W., Severskiy, I., Shahgedanova, M., Wang, M. B., Williamson, S. N., Yang, D. Q., and Mountain Research Initiative EDW Working Group: Elevation-dependent warming in mountain regions of the world, Nat. Clim. Change, 5, 424–430, https://doi.org/10.1038/nclimate2563, 2015.

Pierce, D. W., Barnett, T. P., Hidalgo, H. G., Das, T., Bonfils, C., Santer, B. D., Bala, G., Dettinger, M. D., Cayan, D. R., Mirin, A., Wood, A. W., and Nozawa, T.: Attribution of Declining Western U. S. Snowpack to Human Effects, J. Climate, 21, 6425–6444, https://doi.org/10.1175/2008JCLI2405.1, 2008.

Pifferetti, M., Cat Berro, D., Mercalli, L., Ricciardi, G., and Buffa, A.: La neve nella Pianura Padano-veneta: nuova cartografia 1961–2017, Nimbus, 77, 64–79, 2017.

Pinheiro, J. C. and Bates, D. M.: Mixed-effects models in S and S-PLUS, Springer, New York, 2000.

Prein, A. F. and Gobiet, A.: Impacts of uncertainties in European gridded precipitation observations on regional climate analysis, Int. J. Climatol., 37, 305–327, https://doi.org/10.1002/joc.4706, 2017.

Pulliainen, J., Luojus, K., Derksen, C., Mudryk, L., Lemmetyinen, J., Salminen, M., Ikonen, J., Takala, M., Cohen, J., Smolander, T., and Norberg, J.: Patterns and trends of Northern Hemisphere snow mass from 1980 to 2018, Nature, 581, 294–298, https://doi.org/10.1038/s41586-020-2258-0, 2020.

RCoreTeam: R: A language and Environment for Statistical Computing, R Foundation for Statistical Computing, Vienna, Austria, 2008.

Resch, G., Chimani, B., Koch, R., Schöner, W., and Marty, C.: Homogenization of long-term snow observations, EGU General Assembly 2020, Online, 4–8 May 2020, EGU2020-8807, https://doi.org/10.5194/egusphere-egu2020-8807, 2020.

Salzmann, N. and Mearns, L. O.: Assessing the Performance of Multiple Regional Climate Model Simulations for Seasonal Mountain Snow in the Upper Colorado River Basin, J. Hydrometeorol., 13, 539–556, https://doi.org/10.1175/2011JHM1371.1, 2011.

Scherrer, S. C. and Appenzeller, C.: Swiss Alpine snow pack variability: major patterns and links to local climate and large-scale flow, Clim. Res., 32, 187–199, https://doi.org/10.3354/cr032187, 2006.

Scherrer, S. C., Wüthrich, C., Croci-Maspoli, M., Weingartner, R., and Appenzeller, C.: Snow variability in the Swiss Alps 1864–2009, Int. J. Climatol., 33, 3162–3173, https://doi.org/10.1002/joc.3653, 2013.

Schöner, W., Auer, I., and Böhm, R.: Long term trend of snow depth at Sonnblick (Austrian Alps) and its relation to climate change, Hydrol. Process., 23, 1052–1063, https://doi.org/10.1002/hyp.7209, 2009.

Schöner, W., Koch, R., Matulla, C., Marty, C., and Tilg, A.-M.: Spatiotemporal patterns of snow depth within the Swiss-Austrian Alps for the past half century (1961 to 2012) and linkages to climate change, Int. J. Climatol., 39, 1589–1603, https://doi.org/10.1002/joc.5902, 2019.

Schwaizer, G., Keuris, L., Nagler, T., Derksen, C., Luojus, K., Marin, C., Metsämäki, S., Mudryk, L., Naegeli, K., Notarnicola, C., Salberg, A.-B., Solberg, R., Wiesmann, A., Wunderle, S., Essery, R., Gustafsson, D., Krinner, G., and Trofaier, A.-M.: Towards a long term global snow climate data record from satellite data generated within the Snow Climate Change Initiative, EGU General Assembly 2020, Online, 4–8 May 2020, EGU2020-19228, https://doi.org/10.5194/egusphere-egu2020-19228, 2020.

Steger, C., Kotlarski, S., Jonas, T., and Schär, C.: Alpine snow cover in a changing climate: a regional climate model perspective, Clim. Dynam., 41, 735–754, https://doi.org/10.1007/s00382-012-1545-3, 2013.

Steiger, R. and Stötter, J.: Climate Change Impact Assessment of Ski Tourism in Tyrol, Tourism Geogr., 15, 577–600, https://doi.org/10.1080/14616688.2012.762539, 2013.

Taylor, M. H., Losch, M., Wenzel, M., and Schröter, J.: On the Sensitivity of Field Reconstruction and Prediction Using Empirical Orthogonal Functions Derived from Gappy Data, J. Climate, 26, 9194–9205, https://doi.org/10.1175/JCLI-D-13-00089.1, 2013.

Terzago, S., Cassardo, C., Cremonini, R., and Fratianni, S.: Snow Precipitation and Snow Cover Climatic Variability for the Period 1971–2009 in the Southwestern Italian Alps: The 2008–2009 Snow Season Case Study, Water, 2, 773–787, https://doi.org/10.3390/w2040773, 2010.

Terzago, S., Fratianni, S., and Cremonini, R.: Winter precipitation in Western Italian Alps (1926–2010), Meteorol. Atmos. Phys., 119, 125–136, https://doi.org/10.1007/s00703-012-0231-7, 2013.

Thackeray, C. W., Derksen, C., Fletcher, C. G., and Hall, A.: Snow and Climate: Feedbacks, Drivers, and Indices of Change, Curr. Clim. Chang. Rep., 5, 322–333, https://doi.org/10.1007/s40641-019-00143-w, 2019.

Valt, M. and Cianfarra, P.: Recent snow cover variability in the Italian Alps, Cold Reg. Sci. Technol., 64, 146–157, https://doi.org/10.1016/j.coldregions.2010.08.008, 2010.

Valt, M., Cagnatti, A., Crepaz, A., and Cat Berro, D.: Variazioni Recenti del Manto Nevoso sul Versante Meridionale delle Alpi, Neve e Valanghe, 63, 46–57, available at: https://issuu.com/aineva7/docs/nv63 (last access: 5 March 2021), 2008.

Venables, W. N. and Ripley, B. D.: Modern Applied Statistics with S, 4th edn., Springer-Verlag, New York, 2002.

von Storch, H. and Zwiers, F. W.: Statistical Analysis in Climate Research, Cambridge University Press, Cambridge, 1999.